中国科学院上海应用物理研究所
Shanghai Institute of Applied Physics, Chinese Academy of Sciences

U.S. DEPARTMENT OF ENERGY | Office of Science

BROOKHAVEN NATIONAL LABORATORY

Precise measurement on hypertriton and anti-hypertriton masses with the Heavy Flavor Tracker and the production of triton in Au+Au collisions at STAR

Peng Liu
For the STAR Collaboration
Brookhaven National Laboratory, USA
Shanghai Institute of Applied Physics, CAS, China

Quark Matter 2018 – Venice, Italy
May 13 - 19, 2018

Venezia 2018 Quark Matter

STAR

Motivation and Significance

STAR collaboration, arXix: 1710.00436 [nucl-ex]

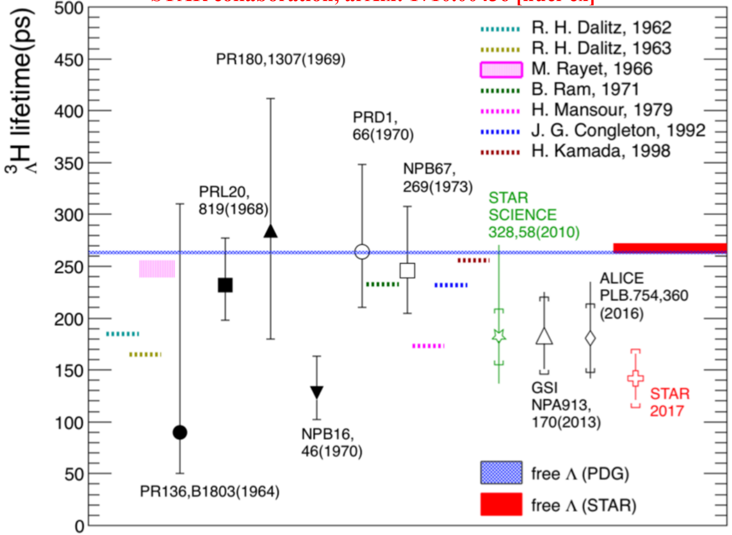

STAR collaboration, Science 328, 58 (2010)

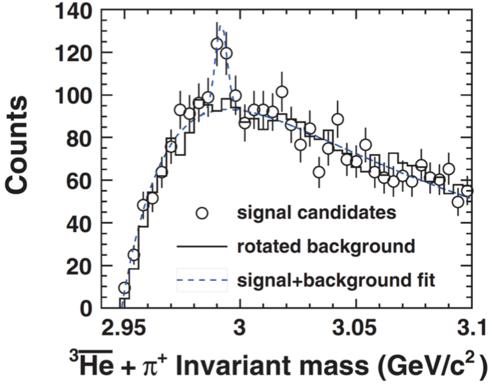

PoS (Hadron2017) 207

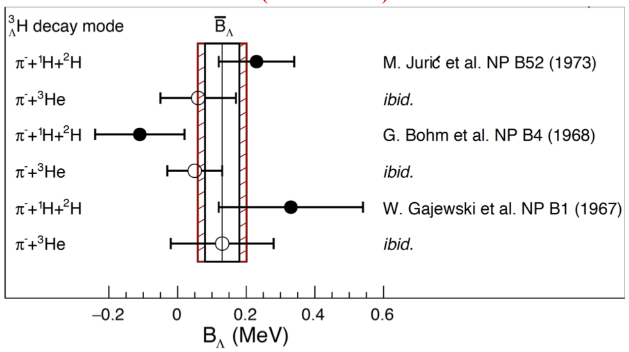

- Hyperon-Nucleon (Y-N) interactions play an important **role in understanding the neutron star and QCD theory** [1, 2, 3].
- Precise measurement of masses of hypertriton ($^{3}_{\Lambda}$H) and anti-hypertriton ($^{3}_{\overline{\Lambda}}\overline{\mathrm{H}}$) provide insight into Y-N interactions and the CPT symmetry.
  1. Mass is more sensitive to the Y-N interactions than the lifetime.
  2. There is no measurement for $^{3}_{\overline{\Lambda}}\overline{\mathrm{H}}$.
- The production of light nuclei is sensitive to the temperature and nucleon phase-space density of the system at freeze-out, hence it could be an excellent tool to explore the QCD properties [4, 5, 6].

[1] R. O. Gomes, V. Dexheimer, S. Schramm, and C. A. Z. Vasconsellos, The Astrophys. J. 808, 8 (2015).
[2] L. L. Lopes and D. P. Menezes, Phys. Rev. C 89, 025805 (2014).
[3] J. Antoniadis et al., Science 340, 448 (2013).
[4] László P. Csernai, Joseph I. Kapusta, Phys. Reps. 131, 223 (1986).
[5] A. Z. Mekjian, Phys. Rev. C 17, 1051 (1978).
[6] Kaijia Sun et al., Phys. Lett. B 774, 103 (2017).

The Solenoidal Tracker at RHIC (STAR)

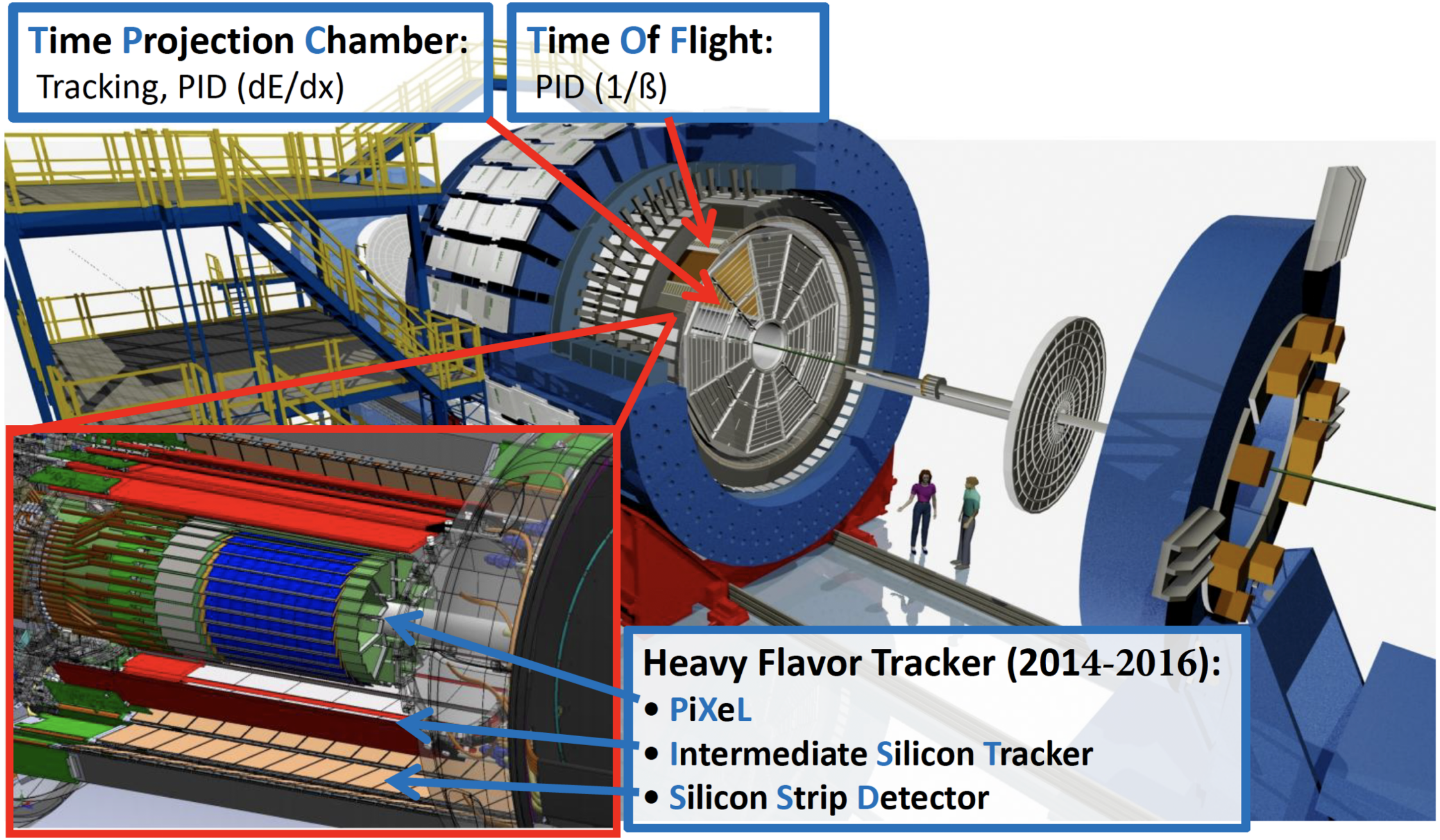

Figure 1. The view of the STAR Detector.

The Heavy Flavor Tracker at STAR (HFT)

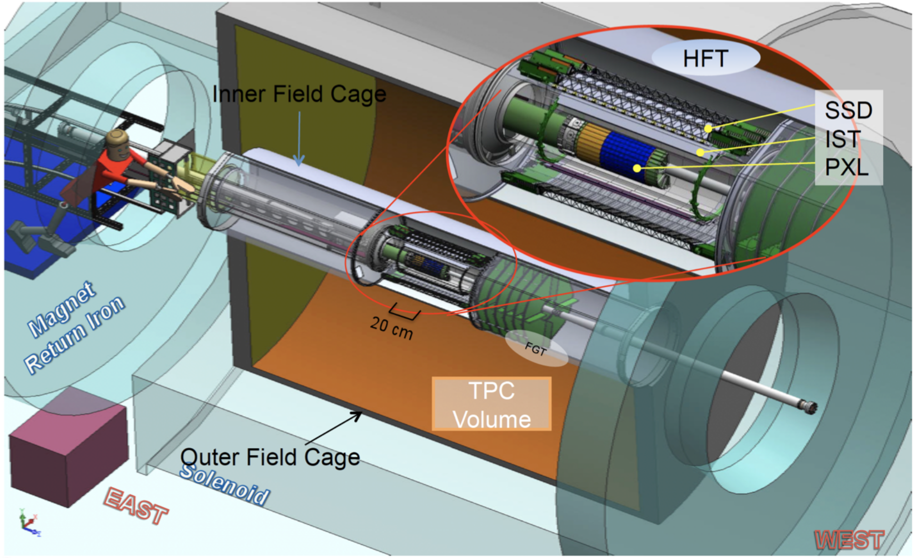

Figure 2. The view of the HFT Detector.

Detector	Radius (cm)	Hit Resolution $(R \times \phi)$ / Z (µm/µm)	Thickness
SSD	22	30/860	1% X_0
IST	14	170/1800	1.32% X_0
PXL	8	6.2/6.2	0.52% X_0
	2.8	6.2/6.2	0.39% X_0

PXL: **PiXeL**
IST: **Intermediate Silicon Tracker**
SSD: **Silicon Strip Detector**

Details on the HFT :
https://drupal.star.bnl.gov/STAR/starnotes/public/sn0600

Taking data:
About 1.2 billion Au+Au collision events in 2014. About 3.4 billion Au+Au collision events in 2016.

TPC → ~1mm → SSD → ~300µm → IST → ~250µm → PXL → < 30µm → vertex

Particle Identification with TPC and TOF

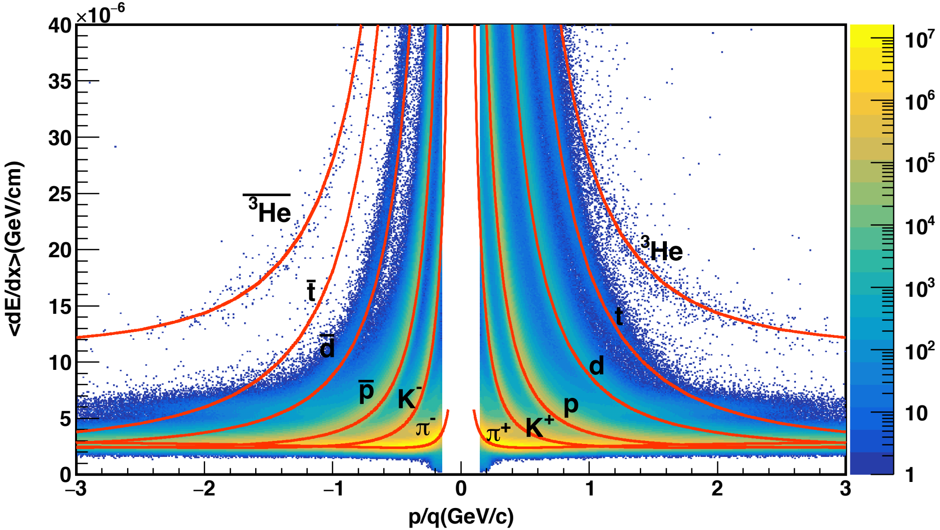

Figure 3. The <dE/dx> versus rigidity measured by TPC in 2014 Au+Au collisions at $\sqrt{s_{NN}}$ = 200 GeV.

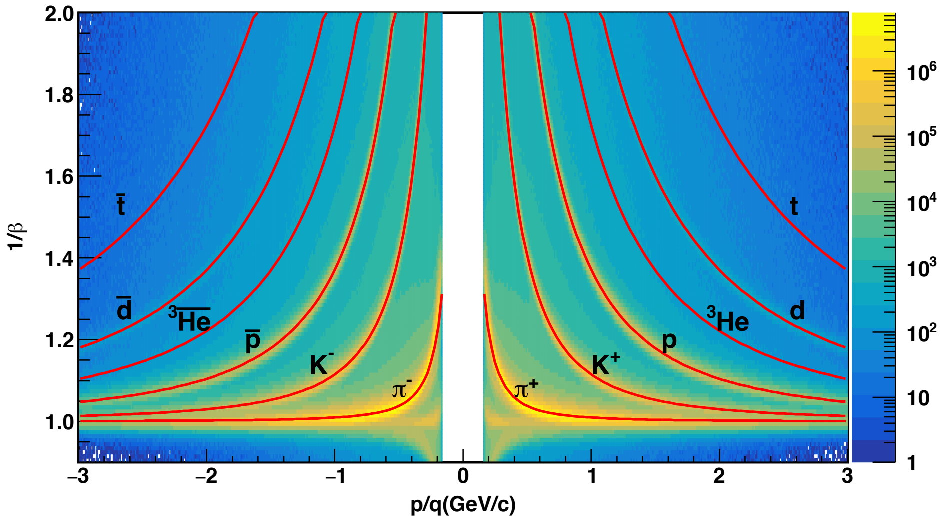

Figure 4. The $1/\beta$ versus rigidity measured by TOF in 2014 Au+Au collisions at $\sqrt{s_{NN}}$ = 200 GeV.

${}^{3}_{\Lambda}$H and ${}^{3}_{\bar{\Lambda}}\bar{\text{H}}$ Reconstruction

$${}^{3}_{\Lambda}H \to {}^{3}He + \pi^{-}$$

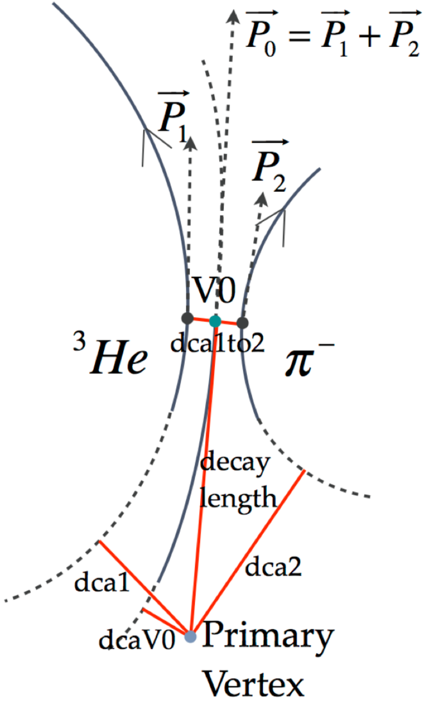

$${}^{3}_{\Lambda}H \to p + \pi^{-} + d$$

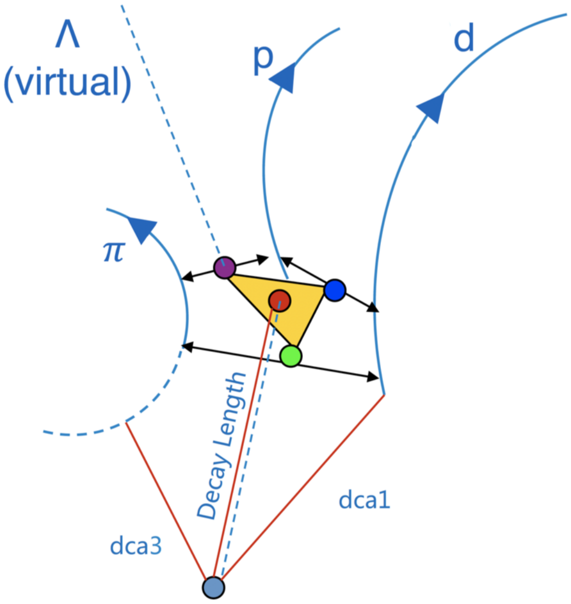

Figure 5. The topology of the ${}^{3}_{\Lambda}$H (${}^{3}_{\bar{\Lambda}}\bar{\text{H}}$) two-body decay and three-body decay.

Because of the high spatial resolution (better than 30 μm) of the HFT, the decay vertex can be determined precisely.

${}^{3}_{\Lambda}$H has many decay channels:

- ✓ Non-meson decay channels:
  - ${}^{3}_{\Lambda}\text{H} \to \text{d} + \text{n}$
  - ${}^{3}_{\Lambda}\text{H} \to \text{p} + \text{n} + \text{n}$
- ✓ Meson decay channels:
  - ${}^{3}_{\Lambda}\text{H} \to {}^{3}\text{He} ({}^{3}\text{H}) + \pi^{-} (\pi^{0})$
  - ${}^{3}_{\Lambda}\text{H} \to \text{d} + \text{p (n)} + \pi^{-} (\pi^{0})$
  - ${}^{3}_{\Lambda}\text{H} \to \text{p} + \text{n} + \text{p (n)} + \pi^{-} (\pi^{0})$

Good PID of charged particles in STAR detector.

Reconstructing ${}^{3}_{\Lambda}$H (${}^{3}_{\bar{\Lambda}}\bar{\text{H}}$) through:

$${}^{3}_{\Lambda}\text{H} \to {}^{3}\text{He} + \pi^{-}$$
$${}^{3}_{\Lambda}\text{H} \to \text{d} + \text{p} + \pi^{-}$$

$^{3}_{\Lambda}$H and $^{3}_{\Lambda}\overline{\text{H}}$ Invariant Masses (before energy loss correction)

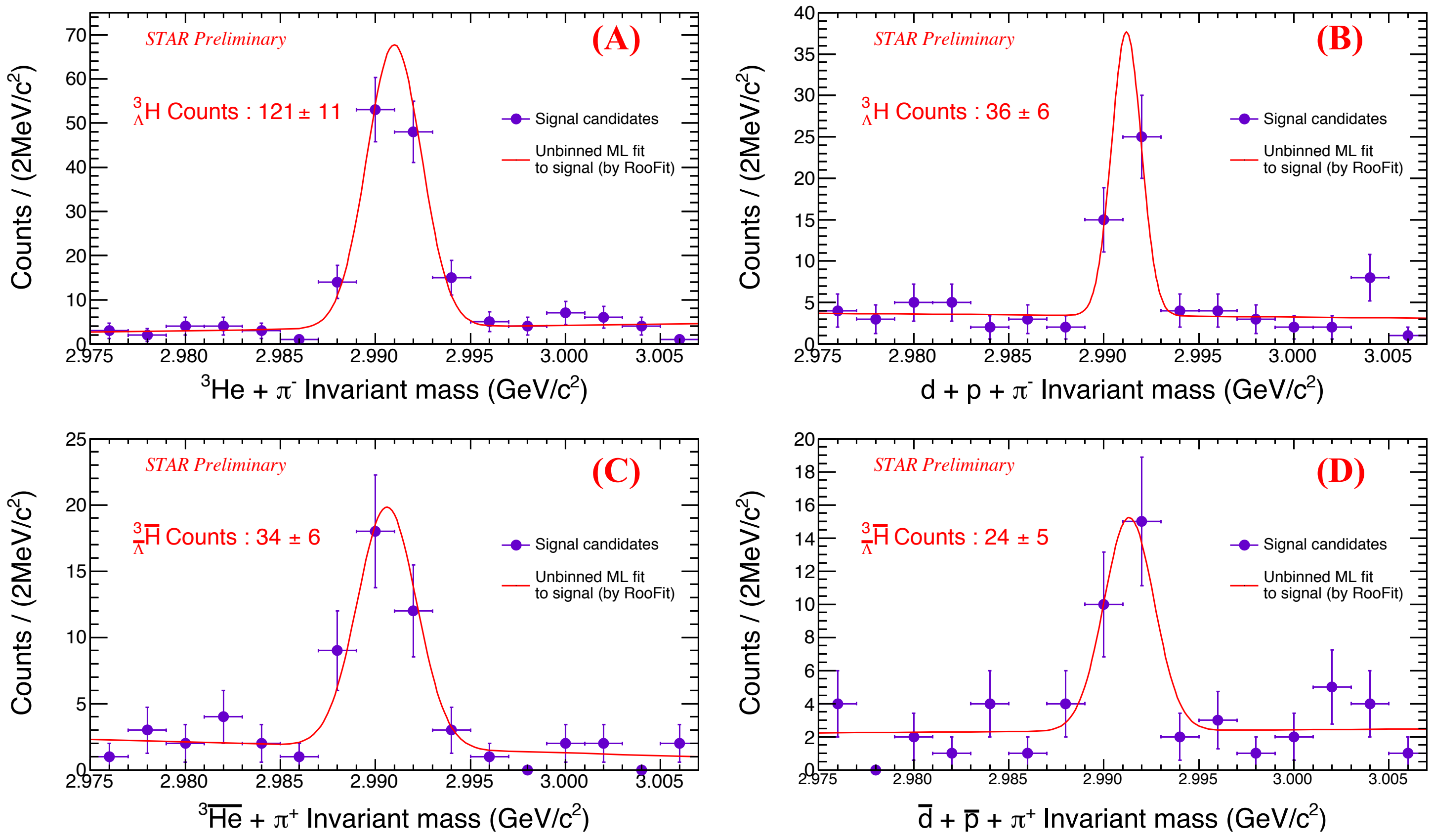

Figure 6. The invariant masses of $^{3}_{\Lambda}$H and $^{3}_{\Lambda}\overline{\text{H}}$ before energy loss correction.

Dataset used:

Au+Au collisions at $\sqrt{s_{NN}}$ = 200 GeV.
Run14: 1.2B events.
Run16: 3.4B events.

$^{3}_{\Lambda}$H and $^{3}_{\Lambda}\overline{\text{H}}$ candidates obtained with excellent S/B ratio.

Fit Function:

$$N_{sig}\left(\frac{1}{\sqrt{2\pi\sigma^2}}e^{-\frac{(x-\mu)^2}{2\sigma^2}}\right) + N_{bkg}(ax+b)$$

${}^{3}_{\Lambda}\mathrm{H}$ and ${}^{3}_{\bar{\Lambda}}\overline{\mathrm{H}}$ Invariant Masses (with energy loss correction)

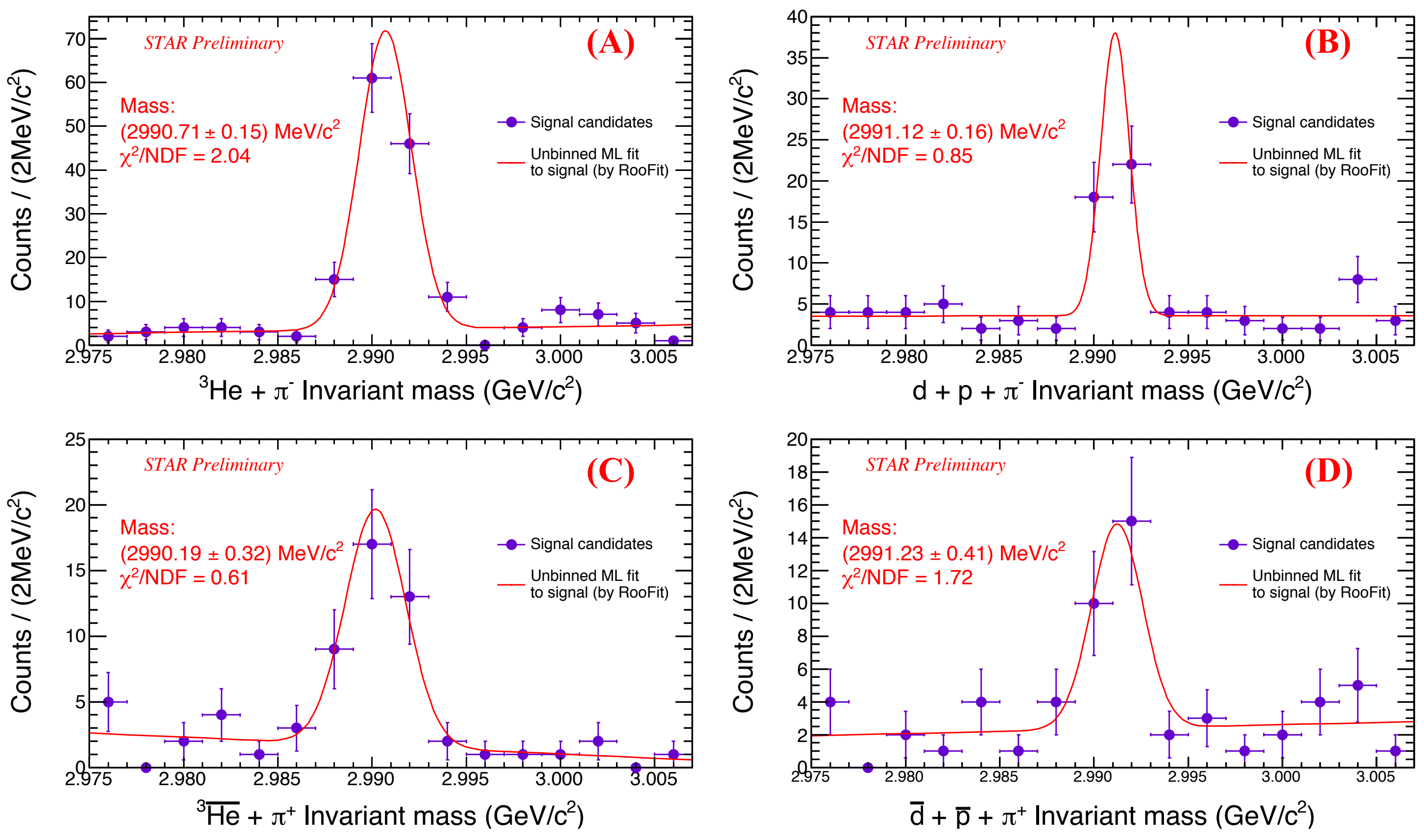

Figure 7. The invariant masses of ${}^{3}_{\Lambda}\mathrm{H}$ and ${}^{3}_{\bar{\Lambda}}\overline{\mathrm{H}}$ with energy loss correction.

Energy loss in the material in front of and in the TPC.

${}^{3}_{\Lambda}\mathrm{H}$ (2-body + 3-body)
2990.90 ± 0.11 (stat.) ± 0.15 (syst.) MeV/c^2

${}^{3}_{\bar{\Lambda}}\overline{\mathrm{H}}$ (2-body + 3-body)
2990.59 ± 0.25 (stat.) ± 0.15 (syst.) MeV/c^2

${}^{3}_{\Lambda}\mathrm{H}$ and ${}^{3}_{\bar{\Lambda}}\overline{\mathrm{H}}$ combined
2990.85 ± 0.10 (stat.) ± 0.15 (syst.) MeV/c^2

Systematical uncertainty source:
- Energy loss correction.
- Different cuts impact.

Fit Function:

$$N_{sig}\left(\frac{1}{\sqrt{2\pi\sigma^2}}e^{-\frac{(x-\mu)^2}{2\sigma^2}}\right)+N_{bkg}(ax+b)$$

Worldwide Binding Energy of ${}^{3}_{\Lambda}H$

Hypertriton B_Λ definition:

$m_\Lambda + m_d - m_{{}^{3}_{\Lambda}H}$

1. Early measurements of B_Λ have large statistical uncertainty due to the limited statistics.

2. The difference between the STAR measurement and the previous measurement is 0.31 ± 0.11 (stat. only) MeV.

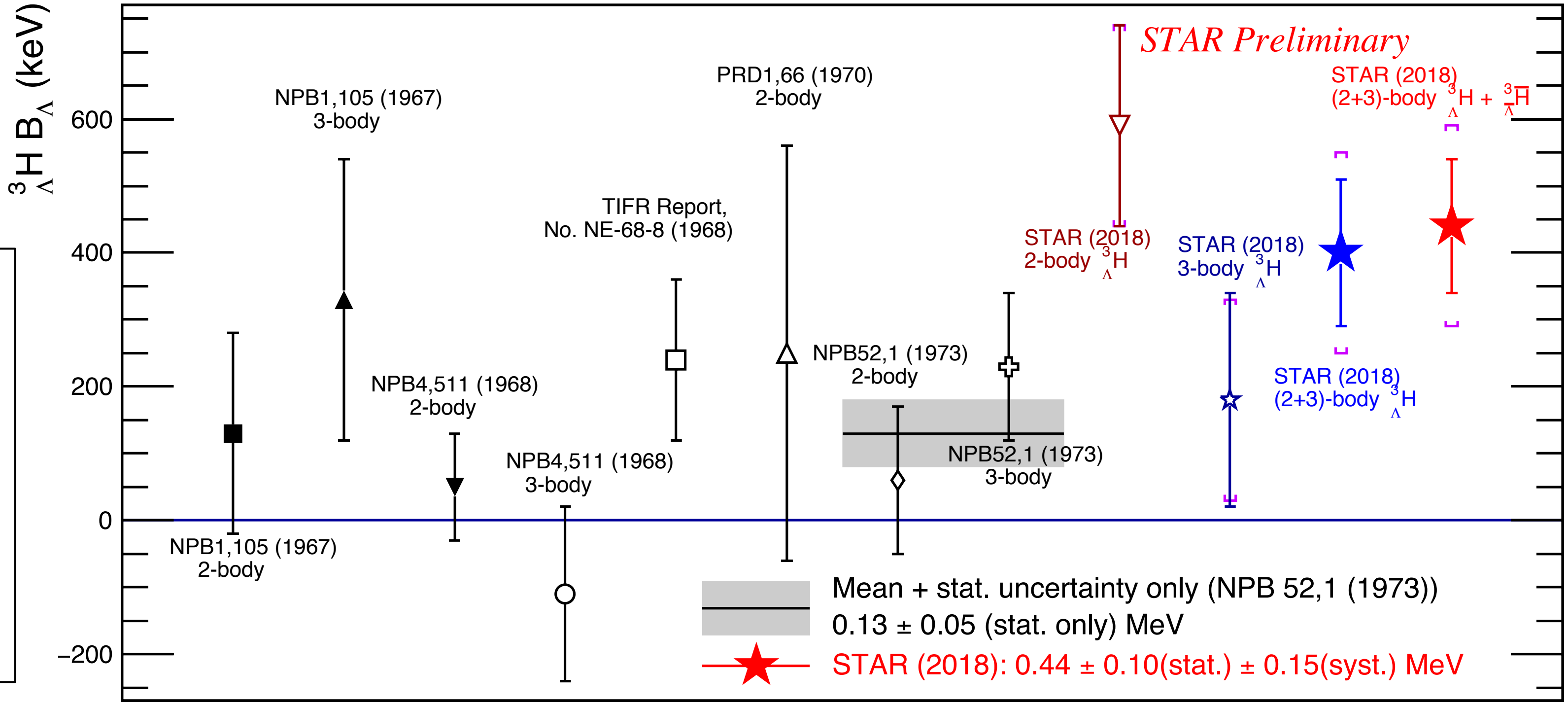

Figure 8. A summary of worldwide binding energy of ${}^{3}_{\Lambda}H$ experimental measurements. The vertical lines are the statistical uncertainty, the brackets are the systematical uncertainty. The gray band is the mean value with its statistical uncertainty measured in 1973.

Mass Difference Between $^{3}_{\Lambda}H$ and $^{3}_{\bar{\Lambda}}\bar{H}$

1. $^{3}_{\Lambda}H$ was discovered in 1952.

2. $^{3}_{\bar{\Lambda}}\bar{H}$ was discovered in 2010 by STAR collaboration [7].

3. Mass difference between $^{3}_{\Lambda}H$ and $^{3}_{\bar{\Lambda}}\bar{H}$ was measured for the first time.

4. The mass difference consistent with CPT prediction.

5. Test of CPT symmetry in the light hypernuclei sector.

$$\left(\frac{\Delta(m/|z|)}{m/|z|}\right)_{d} = (0.9 \pm 0.5\,(\text{stat.}) \pm 1.4\,(\text{syst.}))\times 10^{-4}$$

$$\left(\frac{\Delta(m/|z|)}{m/|z|}\right)_{^{3}He} = (-1.2 \pm 0.9\,(\text{stat.}) \pm 1.0\,(\text{syst.}))\times 10^{-3}$$

$$\left(\frac{\Delta m}{m}\right)_{^{3}_{\Lambda}H} = (1.0 \pm 0.9\,(\text{stat.}) \pm 0.7\,(\text{syst.}))\times 10^{-4}$$

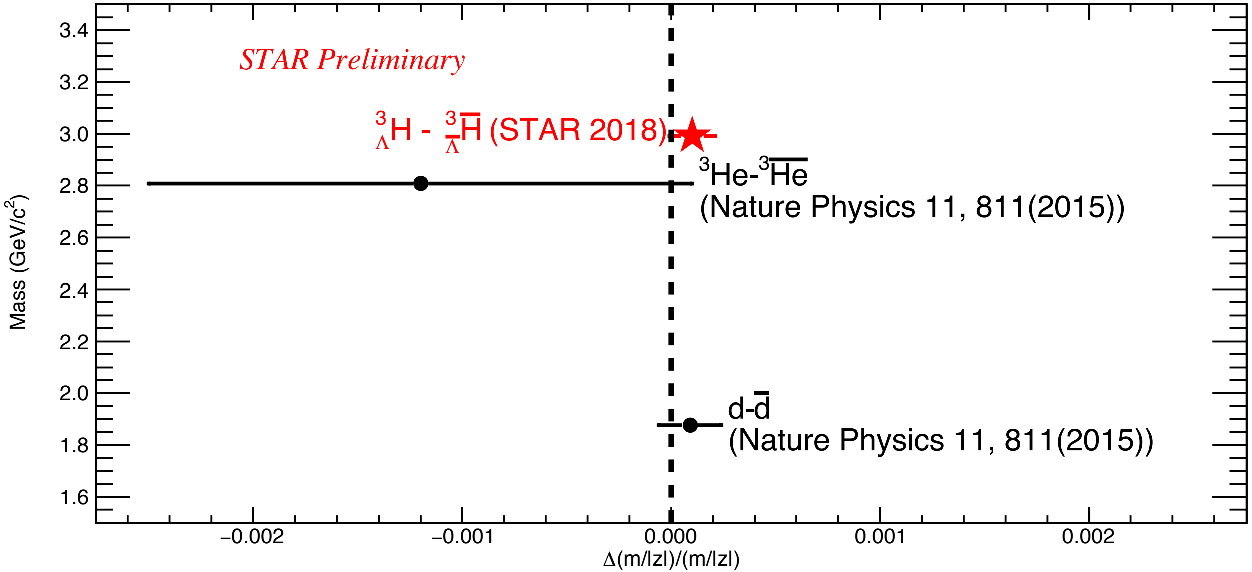

Figure 9. Measurements of the mass-over-charge ratio differences between light nuclei and anti-nuclei. The error bars represent the sum in quadrature of the statistical and systematical uncertainties (standard deviations). Dotted line is the CPT invariance expectation.

[7] B. I. Abelev et al. (STAR Collaboration), Science 328, 58 (2010).

Triton Production – Triton Invariant Yield

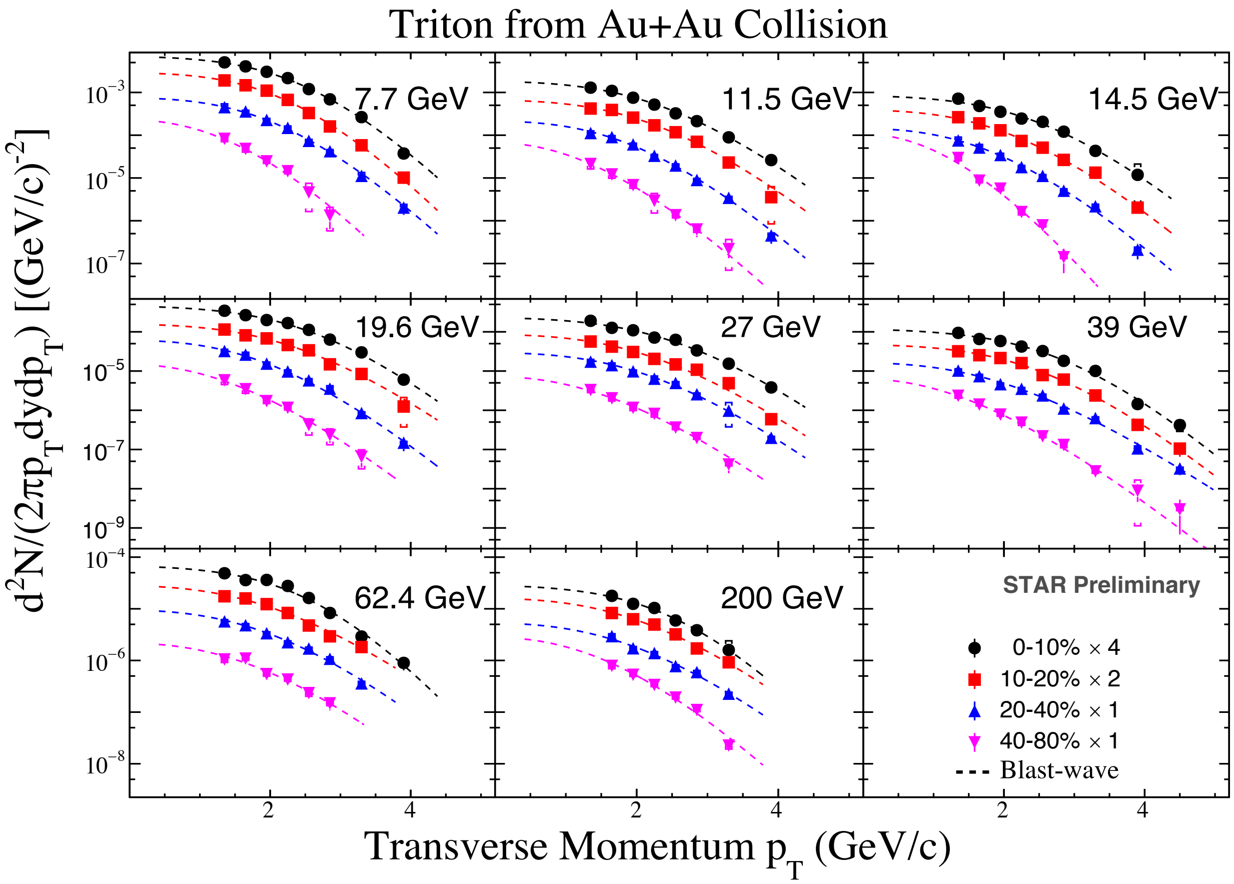

Figure 10. Mid-rapidity (|y|<0.5) transverse momentum distribution of triton in Au+Au collisions at $\sqrt{s_{NN}}$ = 7.7 ~ 200 GeV for 0-10%, 10-20%, 20-40% and 40-80% centralities. The vertical lines represent the statistical uncertainty, the brackets represent the systematical uncertainty.

Blast-wave function:

$$\frac{d^2N}{m_T dm_T dy} \propto \int_0^R r dr m_T I_0\left(\frac{p_T \sinh\rho}{T}\right) K_1\left(\frac{m_T \cosh\rho}{T}\right)$$

Dingwei Zhang, Poster #450.

Triton Production – Coalescence Parameters

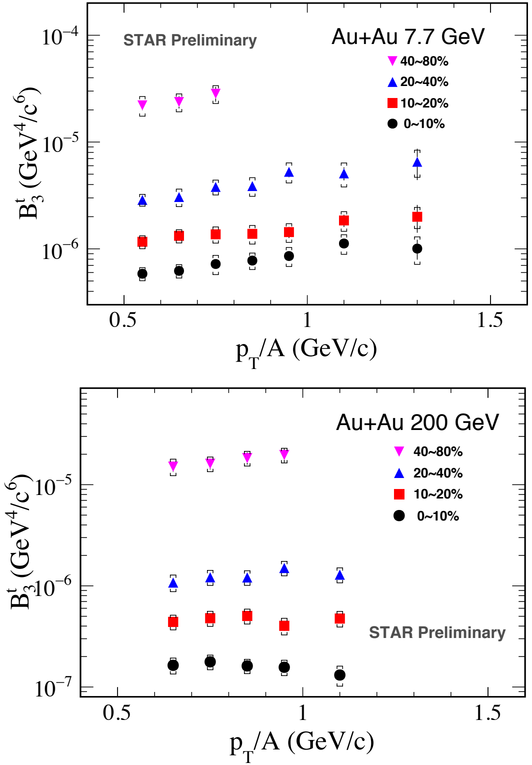

Figure 11. B_3^t versus p_T/A at $\sqrt{s_{NN}}$ = 7.7 and 200 GeV for 0-10%, 10-20%, 20-40% and 40-80% centralities.

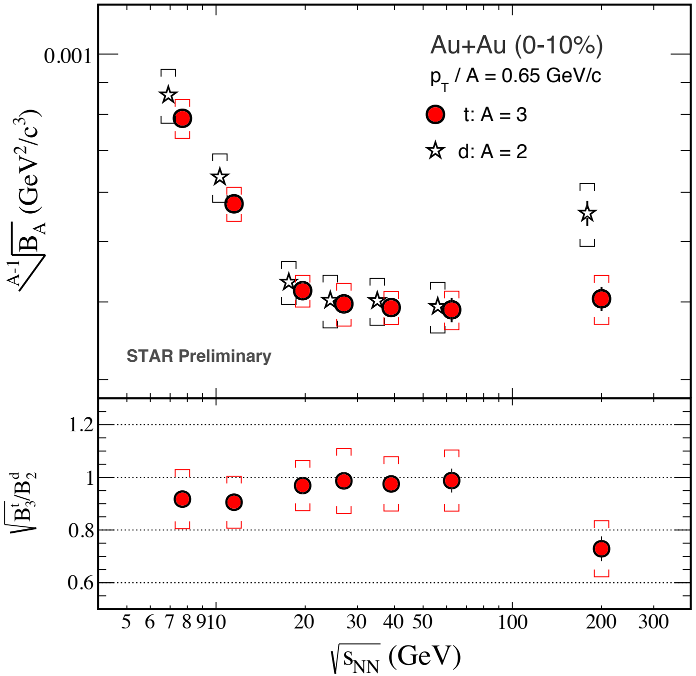

Figure 12. Collision energy dependence of the coalescence parameter $\sqrt{B_3^t}$ and B_2^d. The vertical lines are the statistical uncertainty and the brackets are the systematical uncertainty.

Coalescence formula [4]:

$$E_A \frac{d^3N_A}{dp_A^3} = B_A \left(E_p \frac{d^3N_p}{dp_p^3}\right)^Z \left(E_n \frac{d^3N_n}{dp_n^3}\right)^{A-Z} \approx B_A \left(E_p \frac{d^3N_p}{dp_p^3}\right)^A$$

- ✓ The coalescence parameter B_A reflects the local nucleon density [4].
- ✓ In thermal model, $B_A \propto V_f^{1-A}$, V_f is the freeze-out volume [5].

- ✓ B_3^t decreases (freeze-out volume increases) from peripheral to central collisions.
- ✓ $\sqrt{B_3^t}$ energy dependence is similar to B_2^d below collision energy 200 GeV.

Proton yield is from [8].
Deuteron yield is from [9].

[4] László P. Csernai, Joseph I. Kapusta, Phys. Reps. 131, 223 (1986).
[5] A. Z. Mekjian, Phys. Rev. C 17, 1051 (1978).
[8] STAR Collaboration, arXiv:1707.01988v1 [nucl-ex].
[9] Ning Yu for the STAR Collaboration, Nucl. Phys. A 967, 788 (2017).

Dingwei Zhang, Poster #450.

Triton Production – Neutron Density Fluctuation

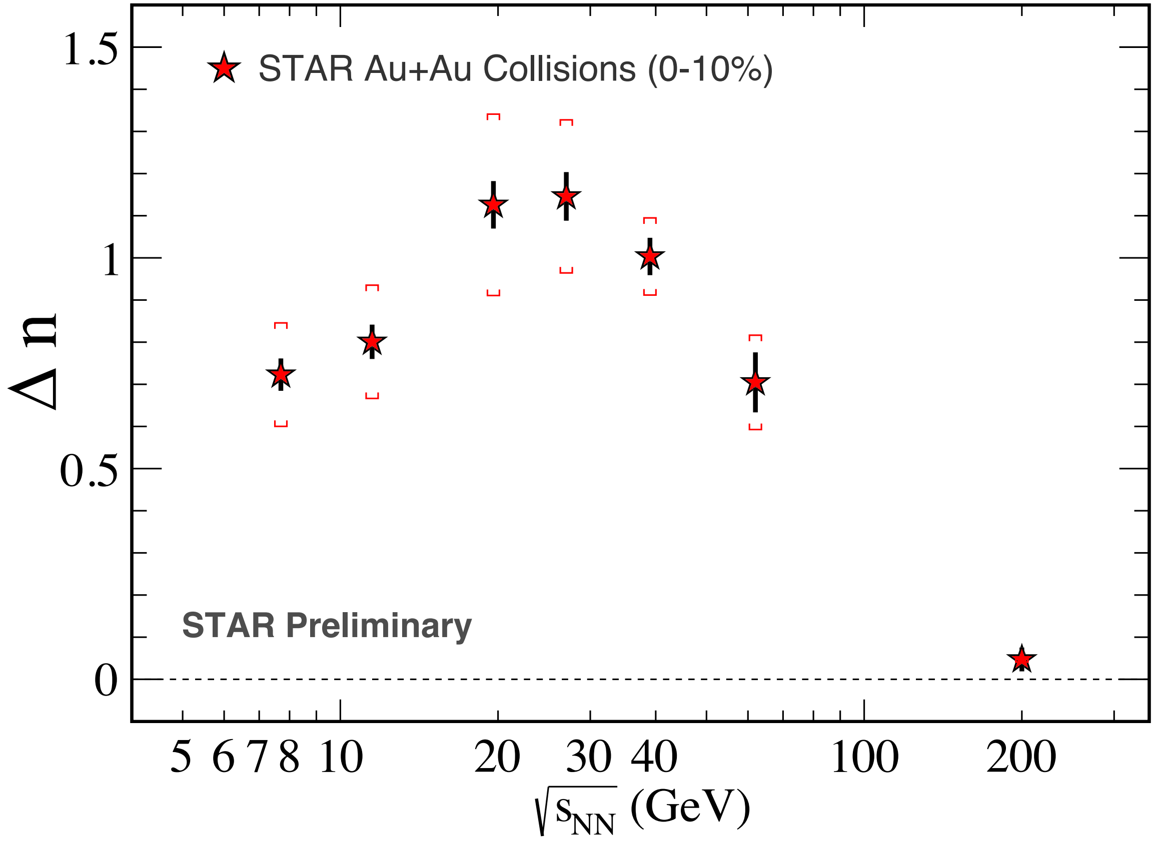

Figure 13. Collision energy dependence of neutron density fluctuation Δn.
The vertical lines are the statistical uncertainty and the brackets are the systematical uncertainty.

Neutron density fluctuation can be expressed as [6]:

$$\Delta n = \langle(\delta n)^2\rangle / \langle n\rangle^2.$$

In our measurement, Δn can be approximated as

$$N_t \cdot N_p / N_d^2 \approx g(1 + \Delta n), \text{ with } g = 0.29.$$

The neutron density fluctuation Δn shows a non-monotonic energy dependence with a peak around 20 - 30 GeV.

Proton yield is from [8].
Deuteron yield is from [9].

[6] Kaijia Sun et al., Phys. Lett. B 774, 103 (2017).
[8] STAR Collaboration, arXiv:1707.01988v1 [nucl-ex].
[9] Ning Yu for the STAR Collaboration, Nucl. Phys. A 967, 788 (2017).

Dingwei Zhang, Poster #450.

Summary

- ✓ The mass and binding energy of hypertriton and anti-hypertriton with STAR Heavy Flavor Tracker were measured.

  ${}^{3}_{\Lambda}\mathrm{H}$ mass: 2990.90 ± 0.11 (stat.) $\pm$ 0.15 (syst.) MeV/c^2.

  ${}^{3}_{\bar{\Lambda}}\overline{\mathrm{H}}$ mass: 2990.59 ± 0.25 (stat.) $\pm$ 0.15 (syst.) MeV/c^2.

  Binding energy (${}^{3}_{\Lambda}\mathrm{H}$ and ${}^{3}_{\bar{\Lambda}}\overline{\mathrm{H}}$ combined): 0.44 ± 0.10 (stat.) $\pm$ 0.15 (syst.) MeV.

- ✓ Mass difference between hypertriton and anti-hypertriton was measured for the first time, which is a test of CPT symmetry in the light hypernuclei sector.

  $$\left(\frac{\Delta m}{m}\right)_{{}^{3}_{\Lambda}\mathrm{H}} = (1.0 \pm 0.9\,(\mathrm{stat.}) \pm 0.7\,(\mathrm{syst.}))\times 10^{-4}.$$

- ✓ Production of triton with the STAR BES-I data was measured.
- ✓ The coalescence parameter B_3 and neutron density fluctuation Δn were extracted from our measurement.

  Energy dependence of Δn shows a non-monotonic behavior with a peak around 20 – 30 GeV.